



Published in final edited form as:

J Tissue Eng Regen Med. 2018 January ; 12(1): 59–69. doi:10.1002/term.2363.

Scaffold-free tissue engineering of lamellar corneal stromal tissue

Fatima N. Syed-Picard, Yiqin Du, Andrew J. Hertsenberg, Rachelle Palchesko, Martha L. Funderburgh, Adam W. Feinberg, and James L. Funderburgh

Abstract

Blinding corneal scarring is predominately treated with allogeneic graft tissue, however, there is a worldwide shortage of donor tissue. In this study, scaffold-free tissue engineering methods were used to generate biomimetic corneal stromal tissue constructs that can be transplanted in vivo without introducing the additional variables associated with exogenous scaffolding. Human corneal stromal stem cells (CSSC) were cultured on substrates with aligned surface microgrooves which directed parallel cell alignment and matrix organization, similar to the organization of native corneal stromal lamella. CSSC produced sufficient matrix to allow manual separation of a tissue sheet from the grooved substrate. These constructs were cellular and collagenous tissue sheets, 4–20 μm thick, containing ECM molecules typical of corneal tissue including types I and V collagen and keratocan. Similar to the native corneal stroma, the engineered corneal tissues contained long parallel collagen fibrils uniform in diameter. After being transplanted into mouse corneal stromal pockets, the engineered corneal stromal tissues became transparent. The human CSSC cells continued to express human corneal stromal matrix molecules. Both in vitro and in vivo, these scaffold-free engineered constructs emulated stromal lamellae of native corneal stromal tissues. Scaffold-free engineered corneal stromal constructs represent a novel autologous, cell-generated biomaterial for use in therapy for corneal blindness.

1. Introduction

The cornea, the anterior most ocular tissue, is composed of a complex structure that facilitates its multiple functions. The cornea acts as physical and biological barrier, protecting the eye. It transmits 99% of incident light unscattered, and provides two-thirds of the refractive power of the eye to focus light onto the retina [1]. The cornea is comprised of three cellular layers, of which the anterior and posterior most tissues are the epithelium and endothelium, respectively. These structures are involved in providing the barrier characteristics of the cornea and in controlling corneal hydration. The corneal stroma is the center-most tissue of the cornea and makes up the bulk of its structure, comprising approximately 90% corneal mass and thickness [2]. The stroma has a highly organized extracellular matrix facilitating its transparency. It is a lamellar structure with each lamella composed of long, tightly packed collagen fibrils that extend the full diameter of the cornea. These fibrils are organized in parallel, uniform in diameter and uniformly spaced to form a lattice-like structure; the direction of the collagen fibrils rotates orthogonally between adjacent lamellae[3]. The highly organized structure of collagen fibrils minimizes light scatter as it passes through the cornea, facilitating corneal transparency[4]. Keratocytes, resident cells of the stroma, maintain its structure in during normal function; however, injury

to the cornea causes keratocytes to differentiate into fibroblasts and deposit a scar tissue [5]. Unlike in healthy stromal tissue, the extracellular matrix in scar tissue is disorganized and opaque, therefore corneal scarring results in loss of visual acuity and sometimes blindness.

Injury, infection and disease cause bilateral corneal blindness in millions of individuals worldwide [6]. The predominant method of treatment, keratoplasty, involves corneal transplantation using allogeneic tissues; however, challenges such as limited tissue availability worldwide and potential graft rejection, prevent successful treatment [7]. Tissue engineering of corneal tissue equivalents tissue to replace damaged or diseased corneal structures could bypass the limitations associated with the current methods of treatment. Ideally, these engineered tissues should be generated from autologous cells avoiding introducing immunological rejection or other adverse biological reactions. Additionally, engineered stromal tissues would need to mimic the characteristic aligned, tightly packed collagen organization and macromolecular composition of native tissues in order to provide the strength and transparency of native stromal tissue.

Traditional tissue engineering involves combination of cells, growth factors, and scaffolding to facilitate formation of three-dimensional tissue equivalents. Exogenous scaffolds used in these methods can strongly influence cell behavior and tissue formation by choice of materials, topography, and mechanical properties [8–10]. During development, however, cells organize appropriate structures without the need for a 3D scaffold. A scaffold-free approach to tissue engineering has been shown useful in production of a number of tissues including skin, periosteum, myocardium, periodontium, and corneal epithelium [11–16]. This technique involves culturing cells as a monolayer, under conditions that promote production of extracellular matrix that forms a robust tissue sheet [17]. Such tissue sheets can be physically removed from substratum or released chemically from thermo-responsive polymer surfaces such as poly(N-isopropylacrylamide) [18]. Application of such a scaffold-free approach to production of corneal stromal tissue sheets could have potential to generate engineered tissue useful for replacement of scarred corneal tissue.

Previous work from our laboratory has described a population of adult stem cells from human corneal stroma which can be expanded in culture without loss of the potential to differentiate to keratocytes [19]. When cultured on a 3D scaffolding of aligned polymeric nanofibers, these corneal stromal stem cells (CSSC) elaborate a ECM with properties similar to that of corneal stroma [20, 21]. In vivo, these cells can restore transparency to opaque corneas in animal models and prevent scar formation after stromal trauma [22, 23]. Furthermore, CSSC can be easily isolated from human biopsy tissues, potentially allowing autologous useage [23]. Although CSSC can generate a stromal ECM in vitro with similar organization of the native corneal stromal tissue, scaffolding used in previous experiments is not transparent and cannot be separated from the cell-generated ECM [20, 21].

In our current study, CSSC were differentiated on a compliant surface formed into parallel microgrooves and found to generate scaffold-free tissue sheets that emulate the highly organized structure of native corneal stromal tissues. These engineered tissues were characterized after in vitro culture, and the ability of these constructs to become transparent, functional stromal tissue in vivo was assessed. This study provides promising data on the

potential use of engineered, scaffold-free corneal stromal tissues as a regenerative therapy to treat corneal blindness.

2. Materials and methods

2.1 Corneal stromal stem cell isolation and culture

CSSC were isolated similar to previously described [19, 23]. Human corneoscleral rims from donors younger than 60 years with less than 5 days of preservation were obtained from the Center for Organ Recovery and Education (www.core.org), after central tissue has been removed for transplantation. The rims were rinsed and residual conjunctiva, Descemet's membrane with endothelial cell layer, and trabecular meshwork were removed. Limbal tissue was dissected from rim, cut into approximately 3 mm segments, and digested in 0.5 mg/ml collagenase L solution overnight at 37 °C. Limbal segments were pipetted repeatedly and digested for an additional 30–40 minutes at 37 °C. Digest was then filtered through a cell strainer and the cells centrifuged at 1500 rpm for 5 minutes. The resulting CSSC were plated onto 25 cm² tissue culture plastic in stem cell growth medium (SCGM) containing 2% (v/v) human serum, DMEM/MCDB-201 (Sigma-Aldrich 6770), AlbuMax (ThermoFisher, #11021029), 0.1 mM ascorbic acid-2-phosphate (Sigma-Aldrich A8960), 1X ITS (ThermoFisher #414-045), 10 ng/mL platelet-derived growth factor (R&D Systems, Minneapolis, MN, #520-BB), 10 ng/mL epidermal growth factor (Sigma-Aldrich E9644), 10⁻⁸ M dexamethasone (Sigma-Aldrich D4902), 100 IU/mL penicillin and 100 ug/mL streptomycin and 50 U/mL gentamycin. CSSC were expanded enzymatically using TrypLe (ThermoFisher) and passaged at clonal density (~1000 cells/cm²). CSSC were used at passage 2–4.

2.2 Micro-patterned substrate preparation

Glass wafers were cleaned with 70% ethanol spin, coated with a 5 µm thick layer of SPR220.3 photoresist (MicroChem Corp) and baked at 115°C for 90 seconds. The photoresist was covered with a transparency photomask, designed in Autocad to have an array of parallel lines 10 µm thick and spaced 10 µm apart, and exposed to UV light for 75 seconds followed by post baking for 90 seconds at 115°C. Regions of photoresist blocked from the UV light were then dissolved using photoresist developer MF26A (MicroChem Corp) to form a grooved mold. Polydimethylsiloxane 184 (PDMS, Down Corning) was mixed at a 10:1 base to curing agent ratio and cast onto the molds to form 1.3 cm × 1.5 cm substrates containing 10 µm wide grooves, spaced 10 µm apart, and approximately 5 µm deep. Dimensions of PDMS substrates were verified by light microscopy using a Nikon TE2000U microscope. To promote cell adhesion, PDMS were coated with fibronectin (50 µg/ml) for 1 hour, rinsed, and UV treated for an additional hour.

2.3 Scaffold-free corneal stromal sheet formation

CSSC were plated onto micro-patterned PDMS substrates at a density of 10,500 cells/cm² in SCGM. After 48 hours, the culture medium was switched to keratocyte differentiation medium (KDM) containing Advanced Dulbecco's Modified Eagle Medium (Gibco) with 1 mM ascorbate-2-phosphate, 10 ng/ml fibroblast growth factor 2 (FGF2; Gibco), and 0.1 ng/ml transforming growth factor beta 3 (TGFβ3; Sigma) [24, 25]. KDM was changed every

2–3 days for 10 days at which point a tissue sheet could be mechanically separated from the substrate. Select tissue sheets were stained with Vybrant DiO (Benzoxazolium, 3-octadecyl-2-[3-(3-octadecyl-2(3H)-benzoxazolylidene)-1-propenyl]-, perchlorate) (ThermoFisher, V-22886), a fluorescent cell membrane tag, by incubation of a solution of 5 μM DiO for 30 minutes at 37°C. Phase contrast and fluorescent images of the cell sheets were acquired using a Nikon TE2000U microscope. Tissue sheets were either fixed and characterized after this *in vitro* culture or used for *in vivo* experiments.

2.5 Two-photon microscopy

Tissue sheets were fixed in 4% paraformaldehyde for 20 minutes and permeabilized using 0.25% Triton X solution for 10 min. Nuclei were stained with 1 μM SYTOX green (ThermoFisher) for 10 min. Two-photon microscopy was performed using an Olympus FV 1000 multi-photon microscope in backscatter mode at wavelength of 830 nm, and the generation of second harmonic signal from aligned collagen was imaged. The samples were imaged through the depth of the sample at a step size of 2 μm .

2.4 *In vivo* cell sheet transplantation

Animal studies were approved by the University of Pittsburgh Institutional Animal Care and Use Committee and carried out according to guidelines provided in the Association for Research in Vision and Ophthalmology Resolution on the Use of Animals in Ophthalmic and Vision Research. Tissue sheets were labelled with either cell membrane dye Vybrant DiO to visualize the implanted cells or 5-(4,6-dichlorotriazinyl) aminofluorescein (DTAF; Sigma D0531) to visualize implanted collagenous matrix throughout the duration of implantation. For DiO labeling, tissue sheets were incubated in a solution of 5 μM DiO for 30 minutes at 37°C, then rinsed twice prior to implantation. For DTAF labelling, tissue sheets were incubated in 1 mg/ml DTAF in 0.2M sodium bicarbonate for 15 minutes at 37°C then washed twice prior to implantation.

After general anesthesia via ketamine/xylazine (IVX Animal Health, Inc., St. Joseph, MO), the eyes of C57BL/6 mice were anesthetized using topical 0.5% proparacaine (Falcon Pharmaceuticals, Fort Worth, TX). An intrastromal pocket was generated using a 27G needle. Tissue sheets were cut using a 2 mm in diameter trephine, and tissue sheets were implanted into the intrastromal pocket using forceps and spread open to lay flat. Mice were euthanized after up to 5 weeks, and eyes were enucleated for further analysis.

2.8 *In Vivo* Imaging and Corneal Opacity Assessment

Mouse corneas with and without implanted tissue sheets were visualized using an Olympus SZX2-ILLT dissecting microscope, 5 weeks after implantation to qualitatively assess corneal clarity and localize either DiO labeled cells or DTAF labeled matrix of the implanted tissue sheet. Mice were anesthetized and stabilized using a three-point stereotactic mouse restrainer, and eyes were lubricated with either a drop of either GenTeal Gel (Alcon) or Gonak (Akorn) prior to imaging.

At 1 and 5 weeks after tissue sheet implantation the mice were anesthetized and the eyes were scanned using optical coherence tomography (OCT) as previously described[23, 26].

Images were acquired using a Bioptigen SD-OCT with an axial resolution of 4 μm and A-scan acquisition rate of 20 kHz $3.5 \times 3.5 \text{ mm}$ 250×250 A-scans. Custom-built macros were used to register and pre-process the volumes, punch a central button from the cornea, and digitally remove the epithelium using FIJI is Just Image J (FIJI) software. MetaMorph (Molecular Devices, Inc version 7.7.8.0) software was used to quantify the average intensity of voxels in the stromal tissue using a uniform threshold for segmentation as a measure of corneal opacity.

2.6 Histology and immunostaining

After *in vitro* culture, tissue sheets were fixed in 4% paraformaldehyde for 20 minutes, embedded paraffin, and cut into 5 μm thick sections. Mouse eyes, 5 weeks after tissue sheet implantation, were immersed in frozen tissue embedding medium (Tissue-Tek O.C.T Compound; Electron Microscopy Sciences), flash frozen in isopentane chilled in liquid nitrogen, and sectioned at a thickness of 12 μm . Prior to staining, sections were fixed in either 2% paraformaldehyde for 10 minutes or chilled acetone for 5 minutes.

Immunostaining was performed using antibodies against human type I collagen (Millipore; catalog # MAB3391), keratocan (Sigma; Catalog no. HPA039321), type V collagen (Clone IE2-E4, Millipore), or human keratocan[22] (kindly provided by Dr. Chia-Yang Liu). Fluorescently tagged secondary antibodies Alexa Fluor 488 anti-mouse IgG, and Alexa Fluor 488 anti-rabbit IgG, or Alexa Fluor 647 anti-rabbit were obtained from ThermoFisher. Staining was performed in parallel without primary antibody as a negative control. DAPI (diamidino-2-phenylindole, 0.5 $\mu\text{g/ml}$) was added to secondary antibody to stain nuclei.

To obtain 3D images of intact stroma, mouse eyes were enucleated and fixed overnight in 2% paraformaldehyde. Corneas were dissected, stained with DAPI. Fluorescent images were obtained from stitched z-stacks of the whole-mounted corneas, acquired on an inverted Olympus IX81 FluoView 1000 confocal microscope with a 20 \times oil (refractive index 0.85) objective. Images were saved in the native OIB format and viewed with Fiji software.

2.7 Transmission electron microscopy

After *in vitro* culture, tissue sheets were fixed in 2.5% glutaraldehyde (Electron Microscopy Sciences) for 1 h, post-fixed in 1% osmium tetroxide (Electron Microscopy Sciences), and dehydrated in graded alcohol washes. The samples were then embedded in Epon (Energy Beam Sciences) and sectioned at 70 nm thickness. The sections were stained with 1% phosphotungstic acid (Sigma Aldrich), pH 3.2 for 10 minutes and visualized with a Jeol 1011 transmission electron microscope at 80 kV.

2.9 Statistical analysis

Corneal stromal light scatter from OCT analyses are presented as averages with error bars representing standard deviation. Independent samples t-tests were used to compare means using GraphPad Prism 4 software and significance was considered at $p < 0.05$.

3. Results

3.1 Scaffold-free engineered stromal lamella-like tissue emulates structure of native tissue

Engineering a tissue with the specialized physical and biological properties of corneal stroma could provide an alternate to allogenic lamellar grafts for treatment of corneal scarring. We have shown that CSSC cells are capable of generating such a tissue, but to date have been unable to obtain material free of scaffolding. To solve this problem CSSC were plated onto a compliant solid substrate that provided topological cues to direct cell and matrix organization. PDMS substrates were generated that contained grooves 10 μm wide, spaced 10 μm apart, and 5 μm deep (Figure 1A and 1B). CSSC cultured on these substrates attached with cell bodies aligned in parallel with the surface grooves (Figure 1C and 1D). Furthermore, as these cells were induced to differentiate to keratocytes, they secreted a collagenous matrix which exhibited parallel collagen fiber alignment as revealed by 2-photon microscopy (Figure 1E). After 10 days of culture in differentiation medium, the cells organized a tissue sheet that could be lifted from the substrate using forceps (Figure 1F).

Transmission electron micrographs of the top view of the tissue sheets show that the matrix contained long, parallel collagen fibers (Figure 2A and 2B). Cross sectional images show that the diameter of the collagen fibers were approximately uniform (Figure 2C and 2D). The average diameter of the collagen fibrils was measured at $30.87 \text{ nm} \pm 6.22$, which is similar to the collagen fibrils found in native human corneal stromal tissues that are reported as approximately 30.8 nm[1]. The size distribution of the collagen fibrils can be seen in Figure 2E.

In addition the structural similarity, with stromal tissue, immunostaining showed the engineered tissue sheets to contain extracellular matrix (ECM) molecules characteristic of native tissues. Type I collagen (Figure 3A), type V collagen (Figure 3B), and keratan (Figure 3C) were found in tissue sheets after *in vitro* culture. These ECM matrix molecules are critical in regulating proper tissue organization in the corneal stroma.

3.2 Scaffold-free engineered stromal lamella-like tissue incorporate into mouse corneal stromal tissues *in vivo*

The scaffold-free engineered tissue sheets were implanted into mouse corneal stromal pockets as a single layer to investigate the effects of the *in vivo* microenvironment on the tissue sheet and assess potential for transparency. After 5 weeks *in vivo*, images of mouse eyes qualitatively appear transparent, and labeled human cells and human matrix originating from the transplanted tissue sheet could be clearly seen in the mouse corneas (Figure 4A–4C). Optical coherence tomography (OCT) was used to quantitatively assess stromal light scatter as an indicator of corneal transparency. One week after tissue sheet transplantation, tissue sheets can still be seen in the OCT scans (Figure 4D–E), however after 5 weeks, tissue sheets could no longer be discerned in the images reconstructed from the scans (Figure 4F). Quantification of the light scatter from these scans indicated a significant increase in stromal light scatter one week after implantation compared control corneas (Figure 4G), but after 5 weeks, the light scatter of corneal stromal tissue containing tissue sheets becomes similar to

those of native un-operated control corneas (Figure 4H). These data show that the engineered tissue sheets become transparent in the mouse corneas.

Whole-mount confocal image stacks of transplanted mouse corneas verified that DiO-labeled, human cells remained in mouse eyes throughout 5 week implantation period (Figure 5a and 5b), and a cross-sectional projection of these stacks showed the cells localized to a linear region of the central stroma where the tissue was implanted (Figure 5c).

Immunostaining of histological sections of the mouse eyes using antibodies specific to human keratocan showed that the human cells delivered in the tissue sheet continued to produce keratocan in vivo (Figure 5d), whereas, the human keratocan was not detected in control eyes lacking tissue sheets (Figure 5e). Controls performed without primary antibody produced no signal (data not shown). These results confirm that scaffold-free tissue sheets delivered to the corneal stroma milieu become transparent, and the stem cells continue to function as differentiated keratocytes in the in vivo microenvironment.

4. Discussion

Tissue engineering of corneal tissues has long thought to have potential to benefit individuals suffering with corneal blindness. Currently allogeneic grafts are used to replace scarred corneal tissue, however, there is a worldwide shortage of donated corneal tissue. Furthermore, over time, the majority of transplanted allogeneic corneal grafts fail [27, 28]. In this study, we found that engineered tissue can be produced by corneal stem cells in an in vitro environment that allows harvest of tissue sheets free of scaffolding. These sheets exhibit the unique structure and composition of native stromal tissues, including parallel collagen fibrils of uniform diameter organized in tight parallel arrays and the corneal-specific proteoglycan keratocan. After in vivo transplantation, the engineered stromal tissue incorporated into native stroma, becoming transparent without eliciting an adverse reaction. We recently reported that CSSC can be isolated from human limbal biopsy tissues [23]. Therefore, the cells capable of producing the engineered stromal tissue can potentially be potentially from patients needing treatment. Scaffold-free engineered stromal tissue therefore represents a biomaterial with significant potential to serve as alternative to allogeneic graft tissue to treat corneal blindness and bypass the limitations of current therapies.

In earlier work we observed that corneal cells are induced to generate a stroma-like engineered tissue by topographical cues from the culture environment, particularly parallel grooves or ridges [20, 21, 23, 29–31]. This stimulus was most effective when cells were cultured on a scaffolding of aligned parallel nanofibers [20, 23]. In that environment, however, integration of the elaborated ECM with the scaffolding prevented obtaining pure engineered tissue. In the current study, we resolved the issue of obtaining scaffold-free engineered stromal tissue by culturing CSSC on a compliant substratum of PDMS, with its apical surface cast into parallel microgrooves during polymerization. The engineered tissue forms with relatively weak attachment to the two-dimensional substratum and can be lifted off manually. We previously showed the usefulness of micropatterned PDMS surfaces in directing behavior of cultured cells [32, 33] but the current study is the first to obtain stem cell-produced stromal ECM free of scaffolding. The PDMS substratum is inexpensive, facile

to reproduce, and can readily be scaled-up, thus this method may be adaptable for biofabrication of corneal tissue on a commercial scale.

The corneal stroma has unique properties, which render it transparent to visible light. These include abundant tightly-packed parallel fibrillar collagen with small uniform fibril diameters, comprised of Types I and V collagen[4]. Corneal transparency is also dependent of the presence of a family of corneal keratan sulfate proteoglycans, of which the corneal-specific protein keratocan makes up about half [4]. ECM produced by CSSC contained the important stromal macromolecules, Type I and V collagens and keratocan (Fig 3) and TEM analysis showed the collagen fibrils to be organized in a manner similar to that in the human stroma. The diameter of the fibrils was similar to that of native human stroma, approximately 30.9 nm suggesting this material has the potential to function as stromal tissue.

In addition to requiring specialized matrix composition and structure, transparency of the stroma only occurs in the context a specific level of hydration provided by the pumping function of the corneal endothelium. Thus it is not possible to assess the functional transparency of stromal tissue *ex vivo*. Generation of tissue sheets free from opaque polymeric scaffolding, made it possible for the first time to test ECM made by CSSC for functional transparency by implanting them into stromal pockets of living eyes. The engineered tissue sheets were not transparent immediately *in vivo* but became transparent over time (Fig 4). This suggests that the corneal milieu may induce some reorganization of the ECM before transparency occurs. Such reorganization could involve collagen remodeling, however, by pre-labeling collagen in with DTAF, we know that original collagen from the tissue construct remained in transparent stroma 5 weeks after implantation (Fig 4). In transmission electron micrographs of mouse corneas 5 weeks after implantation, implanted tissue was indistinguishable from the host mouse tissue (data not shown), indicating that collagen of the engineered tissues had fully incorporated into the surrounding mouse tissue. The human cells delivered via the scaffold-free tissue sheets, however, clearly remained in the tissue at 5 weeks continued to produce human keratocan (Fig 5). These data further support the idea that scaffold-free engineered stromal tissues are capable of fully integrating into the stroma and adopting functional native structures.

A number of reports have demonstrated synthesis of stroma-like matrix by corneal cells *in vitro* [31, 34–41]. Many of these studies have used mesenchymal cells expanded from corneal stroma in serum-containing media; *i.e.*, corneal fibroblasts. Although some of these studies report the production of a stroma-like matrix from corneal fibroblasts, several observations support the superiority of a stem-cell based approach to this task. Fibroblasts do not maintain the ability to adopt a keratocyte phenotype through many population doublings [42]. This results in the need to use low-passage cells, available in rather limited amounts, or to use cells from more than one donor. We have successfully expanded CSSC through >20 doublings without loss of phenotype, so that CSSC from a single donor has the potential to produce keratocytes sufficient to make >10⁴ corneas [19, 24]. Our previous studies comparing fibroblasts and CSSC show that fibroblast-produced ECM lacks some of the critical molecular components of stroma, particularly keratan sulfate [29, 30]. Most importantly is the growing body of evidence that mesenchymal stem cells have immunosuppressive properties. We previously found human that CSSC elicit little or no

inflammatory response when introduced into the mouse cornea, but that corneal fibroblasts produce T-cell infiltration, haze and rejection [22]. The scaffold-free tissue sheets in this study were generated from human CSSC and the resulting constructs were implanted into immunocompetent mice, but the engineered tissues did not elicit detectable immune response from the host (data not shown). Extrapolation of these results to a human model suggests that corneal tissues produced by CSSC may be better tolerated immunologically than tissues produced by fibroblasts. Although use of autologous cells may be best, in cases where autologous cells are not available, stromal tissue produced by CSSC allogenic tissues may be a better second option.

5. Conclusions

Scaffold-free tissue sheets were generated from CSSC that reproduced the highly organized structure and molecular composition of native corneal stromal lamellae. After transplantation into corneal stromal pockets, the engineered tissue sheets incorporated into surrounding tissues and became transparent without eliciting any adverse reaction. The data support the idea that scaffold-free engineered stromal constructs could be used as an autologous, cell-generated biomaterial for regenerative therapies to treat corneal blindness.

Acknowledgments

The authors would like to thank the Mr. Gregory Gibson, Ms. Mara Grove, and Mr. Jonathan Franks from the University of Pittsburgh, Center for Biological Imaging for help with 2-photon microscopy and transmission electron microscopy. The authors also thank Ms. Katherine Davoli and Ms. Kira Lathrop for helping prepare histological tissue sections, and help with imaging, respectively. The authors thank Dr. David Birk and Ms. Sheila Adams for transmission electron microscopy work referred to in this manuscript on mouse eyes containing tissue sheets. This research was supported by National Institutes of Health Grants EY016415 (JLF), EY009368 (JLF), P30-EY008098, Research to Prevent Blindness, and the Eye and Ear Foundation of Pittsburgh. FNS is an OTERO fellow of the Louis J Fox Center for Vision Restoration.

References

1. Meek KM, Leonard DW. Ultrastructure of the corneal stroma: a comparative study. *Biophys J.* 1993; 64:273–80. [PubMed: 8431547]
2. Levin, LA., Adler, FH. Adler's physiology of the eye : clinical application. 11. Edingburg: Saunders/Elsevier; 2011.
3. Smolin, G., Foster, CS., Azar, DT., Dohlman, CH. Smolin and Thoft's the cornea : scientific foundations and clinical practice. 4. Philadelphia: Lippincott Williams & Wilkins; 2005.
4. Hassell JR, Birk DE. The molecular basis of corneal transparency. *Exp Eye Res.* 2010; 91:326–35. [PubMed: 20599432]
5. Fini ME. Keratocyte and fibroblast phenotypes in the repairing cornea. *Progress in retinal and eye research.* 1999; 18:529–51. [PubMed: 10217482]
6. Whitcher JP, Srinivasan M, Upadhyay MP. Corneal blindness: a global perspective. *Bulletin of the World Health Organization.* 2001; 79:214–21. [PubMed: 11285665]
7. Williams KA, Esterman AJ, Bartlett C, Holland H, Hornsby NB, Coster DJ. How effective is penetrating corneal transplantation? Factors influencing long-term outcome in multivariate analysis. *Transplantation.* 2006; 81:896–901. [PubMed: 16570014]
8. LeGeros RZ. Calcium phosphate-based osteoinductive materials. *Chem Rev.* 2008; 108:4742–53. [PubMed: 19006399]
9. Engler AJ, Sen S, Sweeney HL, Discher DE. Matrix elasticity directs stem cell lineage specification. *Cell.* 2006; 126:677–89. [PubMed: 16923388]

10. Clark P, Connolly P, Curtis AS, Dow JA, Wilkinson CD. Cell guidance by ultrafine topography in vitro. *J Cell Sci.* 1991; 99(Pt 1):73–7. [PubMed: 1757503]
11. Liu Y, Luo H, Wang X, Takemura A, Fang YR, Jin Y, et al. In vitro construction of scaffold-free bilayered tissue-engineered skin containing capillary networks. *Biomed Res Int.* 2013; 2013:561410. [PubMed: 23607091]
12. Na S, Zhang H, Huang F, Wang W, Ding Y, Li D, et al. Regeneration of dental pulp/dentine complex with a three-dimensional and scaffold-free stem-cell sheet-derived pellet. *Journal of tissue engineering and regenerative medicine.* 2013
13. Chang C-H, Chen C-H, Liu H-W, Whu S-W, Chen S-H, Tsai C-L, et al. Bioengineered periosteal progenitor cell sheets to enhance tendon-bone healing in a bone tunnel. *Biomed J.* 2012; 35:473–80. [PubMed: 23442360]
14. Owaki T, Shimizu T, Yamato M, Okano T. Cell sheet engineering for regenerative medicine: current challenges and strategies. *Biotechnol J.* 2014; 9:904–14. [PubMed: 24964041]
15. DuRaine GD, Brown WE, Hu JC, Athanasiou KA. Emergence of scaffold-free approaches for tissue engineering musculoskeletal cartilages. *Ann Biomed Eng.* 2015; 43:543–54. [PubMed: 25331099]
16. Masuda S, Shimizu T. Three-dimensional cardiac tissue fabrication based on cell sheet technology. *Adv Drug Deliv Rev.* 2015
17. See EY-S, Toh SL, Goh JCH. Multilineage potential of bone-marrow-derived mesenchymal stem cell sheets: implications for tissue engineering. *Tissue Eng Part A.* 2010; 16:1421–31. [PubMed: 19951089]
18. Akiyama Y, Kikuchi A, Yamato M, Okano T. Ultrathin poly(N-isopropylacrylamide) grafted layer on polystyrene surfaces for cell adhesion/detachment control. *Langmuir.* 2004; 20:5506–11. [PubMed: 15986693]
19. Du Y, Funderburgh ML, Mann MM, SundarRaj N, Funderburgh JL. Multipotent stem cells in human corneal stroma. *Stem Cells.* 2005; 23:1266–75. [PubMed: 16051989]
20. Wu J, Du Y, Watkins SC, Funderburgh JL, Wagner WR. The engineering of organized human corneal tissue through the spatial guidance of corneal stromal stem cells. *Biomaterials.* 2012; 33:1343–52. [PubMed: 22078813]
21. Wu J, Du Y, Mann MM, Yang E, Funderburgh JL, Wagner WR. Bioengineering organized, multilamellar human corneal stromal tissue by growth factor supplementation on highly aligned synthetic substrates. *Tissue Eng Part A.* 2013; 19:2063–75. [PubMed: 23557404]
22. Du Y, Carlson EC, Funderburgh ML, Birk DE, Pearlman E, Guo N, et al. Stem cell therapy restores transparency to defective murine corneas. *Stem Cells.* 2009; 27:1635–42. [PubMed: 19544455]
23. Basu S, Hertsensberg AJ, Funderburgh ML, Burrow MK, Mann MM, Du Y, et al. Human limbal biopsy-derived stromal stem cells prevent corneal scarring. *Sci Transl Med.* 2014; 6:266ra172.
24. Du Y, Sundarraj N, Funderburgh ML, Harvey SA, Birk DE, Funderburgh JL. Secretion and organization of a cornea-like tissue in vitro by stem cells from human corneal stroma. *Invest Ophthalmol Vis Sci.* 2007; 48:5038–45. [PubMed: 17962455]
25. Wu J, Du Y, Mann MM, Yang E, Funderburgh J, Wagner WR. Bioengineering Organized, Multi-Lamellar Human Corneal Stromal Tissue by Growth Factor Supplementation on Highly Aligned Synthetic Substrates. *Tissue engineering Part A.* 2013
26. Boote C, Du Y, Morgan S, Harris J, Kamma-Lorger CS, Hayes S, et al. Quantitative assessment of ultrastructure and light scatter in mouse corneal debridement wounds. *Invest Ophthalmol Vis Sci.* 2012; 53:2786–95. [PubMed: 22467580]
27. Kelly TL, Williams KA, Coster DJ. Corneal transplantation for keratoconus: a registry study. *Arch Ophthalmol.* 2011; 129:691–7. [PubMed: 21320951]
28. Coster DJ, Williams KA. The impact of corneal allograft rejection on the long-term outcome of corneal transplantation. *Am J Ophthalmol.* 2005; 140:1112–22. [PubMed: 16376660]
29. Wu J, Rnjak-Kovacina J, Du Y, Funderburgh ML, Kaplan DL, Funderburgh JL. Corneal stromal bioequivalents secreted on patterned silk substrates. *Biomaterials.* 2014; 35:3744–55. [PubMed: 24503156]

30. Wu J, Du Y, Mann MM, Funderburgh JL, Wagner WR. Corneal stromal stem cells versus corneal fibroblasts in generating structurally appropriate corneal stromal tissue. *Exp Eye Res.* 2014; 120:71–81. [PubMed: 24440595]
31. Karamichos D, Funderburgh ML, Hutcheon AEK, Zieske JD, Du Y, Wu J, et al. A role for topographic cues in the organization of collagenous matrix by corneal fibroblasts and stem cells. *PLoS One.* 2014; 9:e86260. [PubMed: 24465995]
32. Palchesko RN, Lathrop KL, Funderburgh JL, Feinberg AW. In vitro expansion of corneal endothelial cells on biomimetic substrates. *Sci Rep.* 2015; 5:7955. [PubMed: 25609008]
33. Palchesko RN, Zhang L, Sun Y, Feinberg AW. Development of polydimethylsiloxane substrates with tunable elastic modulus to study cell mechanobiology in muscle and nerve. *PLoS One.* 2012; 7:e51499. [PubMed: 23240031]
34. Karamichos D, Hutcheon AE, Zieske JD. Transforming growth factor-beta3 regulates assembly of a non-fibrotic matrix in a 3D corneal model. *Journal of tissue engineering and regenerative medicine.* 2011; 5:e228–38. [PubMed: 21604386]
35. Guillemette MD, Cui B, Roy E, Gauvin R, Giasson CJ, Esch MB, et al. Surface topography induces 3D self-orientation of cells and extracellular matrix resulting in improved tissue function. *Integr Biol (Camb).* 2009; 1:196–204. [PubMed: 20023803]
36. Mimura T, Amano S, Yokoo S, Uchida S, Yamagami S, Usui T, et al. Tissue engineering of corneal stroma with rabbit fibroblast precursors and gelatin hydrogels. *Mol Vis.* 2008; 14:1819–28. [PubMed: 18852871]
37. Boulze Pankert M, Goyer B, Zaguia F, Bareille M, Perron M-C, Liu X, et al. Biocompatibility and functionality of a tissue-engineered living corneal stroma transplanted in the feline eye. *Invest Ophthalmol Vis Sci.* 2014; 55:6908–20. [PubMed: 25277228]
38. Karamichos D, Rich CB, Zareian R, Hutcheon AE, Ruberti JW, Trinkaus-Randall V, et al. TGF-beta3 stimulates stromal matrix assembly by human corneal keratocyte-like cells. *Invest Ophthalmol Vis Sci.* 2013
39. Karamichos D, Guo XQ, Hutcheon AE, Zieske JD. Human corneal fibrosis: an in vitro model. *Invest Ophthalmol Vis Sci.* 2010; 51:1382–8. [PubMed: 19875671]
40. Ruberti JW, Zieske JD. Prelude to corneal tissue engineering - gaining control of collagen organization. *Progress in retinal and eye research.* 2008; 27:549–77. [PubMed: 18775789]
41. Ren R, Hutcheon AE, Guo XQ, Saeidi N, Melotti SA, Ruberti JW, et al. Human primary corneal fibroblasts synthesize and deposit proteoglycans in long-term 3-D cultures. *Developmental dynamics : an official publication of the American Association of Anatomists.* 2008; 237:2705–15. [PubMed: 18624285]
42. Long CJ, Roth MR, Tasheva ES, Funderburgh M, Smit R, Conrad GW, et al. Fibroblast growth factor-2 promotes keratan sulfate proteoglycan expression by keratocytes in vitro. *J Biol Chem.* 2000; 275:13918–23. [PubMed: 10788517]

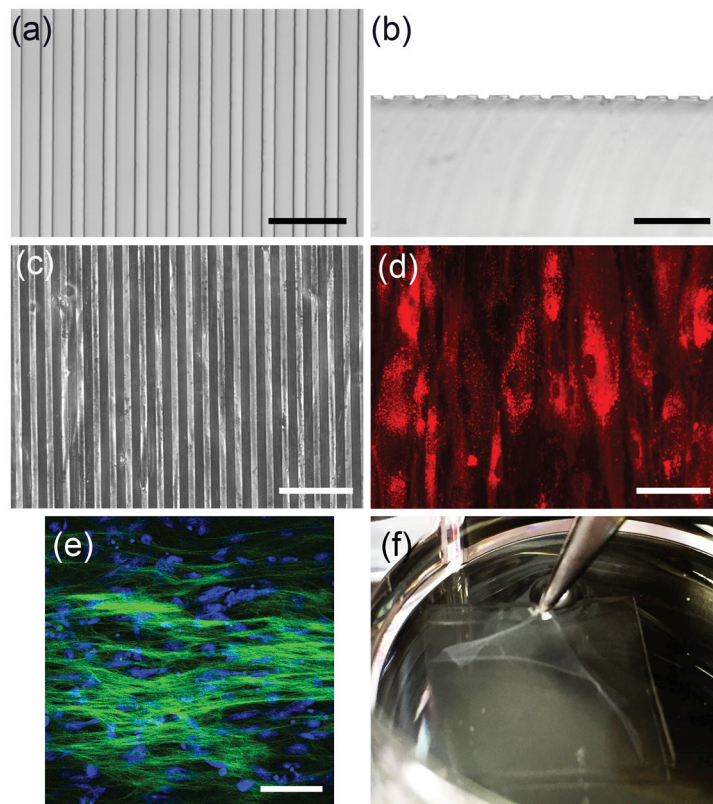


Figure 1. Formation of scaffold-free tissue sheet with parallel cell and matrix organization

Light micrographs of (a) top view and (b) cross sectional view of the PDMS substrate show grooves approximately $10\ \mu\text{m}$ wide, $10\ \mu\text{m}$ apart, and $5\ \mu\text{m}$ deep. (c) Phase contrast image shows CSSC cultured on the grooved substrate. (d) For better visualization, CSSC were labeled with DiI (red) and cultured on grooved substrate. (e) Two-photon micrograph of 10-day cultures of CSSC on grooved substrates in keratocyte differentiation medium (KDM) shows deposition of parallel organized collagenous matrix (green). Nuclei (blue) were stained by SYTOX-green (blue). (f) After 10 days of culture a robust tissue sheet is formed that can be separated from the substrate using forceps. Scale bars: (a) and (b) = $50\ \mu\text{m}$, (c)–(e) = $100\ \mu\text{m}$

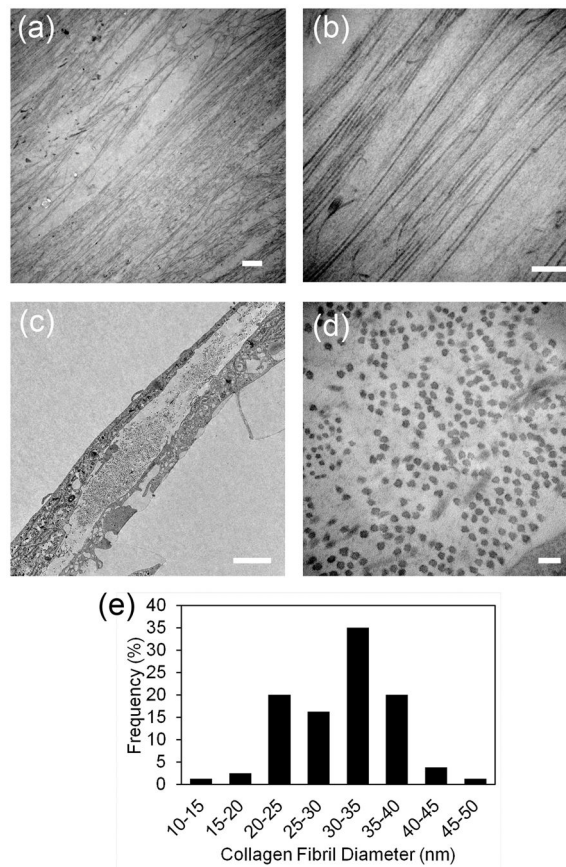


Figure 2. Transmission electron microscopy of scaffold-free tissue sheets generated in vitro Scaffold-free tissue sheets harvested after 12 days culture in KDM were fixed and imaged by TEM as described in Methods. (a) Lower and (b) higher magnification images of the top view of scaffold-free tissue sheets shows that the constructs contain long, parallel organized collagen fibrils. (c) Lower and (d) higher magnification images of engineered corneal stroma tissues in cross section show collagen fibrils are approximately uniform in diameter. (e) Size distribution of collagen fibril diameters as measured from TEM images of cross section of engineered tissues show that collagen fibril diameter are similar to the collagen fibril diameter seen in native, human corneal stromal tissue. Scale bars: (a) = 2 μm , (b) = 500 nm, (c) 2 μm , and (d) = 100 nm

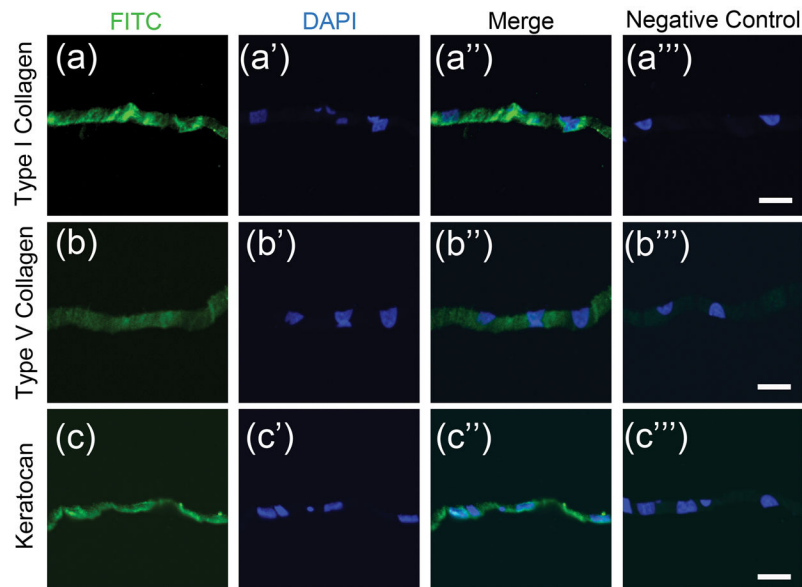


Figure 3. Immunostaining of scaffold-free tissue sheets produced in vitro

Paraffin sections of scaffold-free tissue sheets produced after 12 days culture in KDM were immunostained as described in Methods. (a) Presence of for type I collagen (green) was detected in the matrix of scaffold-free tissue sheets, (a') with corresponding nuclear DAPI stain (blue), (a'') merged image of (a) and (a'), and (a''') corresponding merged image of negative control. (b) Type V collagen expression was seen in engineered tissue sheets with (b') corresponding nuclear DAPI stain (blue), (b'') merged image of (b) and (b'), and (b''') corresponding merged image of negative control. (c) Keratocan expression was detected in scaffold-free tissue sheets, with (c') corresponding nuclear DAPI stain (blue), (c'') merged image of (c) and (c'), and (c''') corresponding merged image of negative control. Scale bars: 20 μm

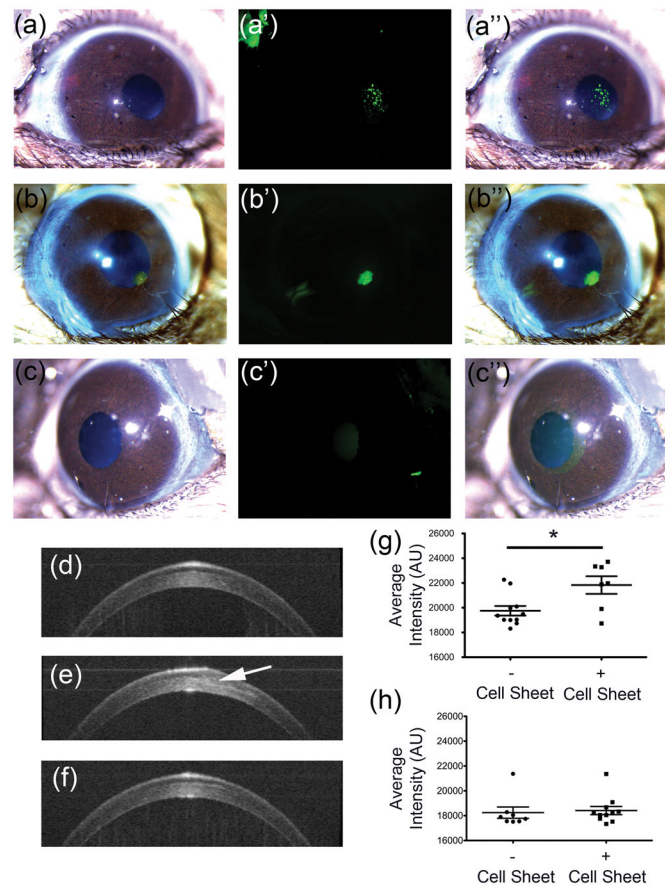


Figure 4. Histological analysis of scaffold-free tissue sheets in mouse stromal pockets in vivo Mouse eyes were imaged in vivo after lamellar transplantation of scaffold-free tissue sheets as described in Methods. (a) Light micrograph image of mouse eye containing scaffold-free tissue sheet with DiO-labeled cells, (a') with corresponding fluorescent image showing human cells (green), and (a'') the merged image of (a) and (a'). (b) Light micrograph image of mouse eye containing scaffold-free tissue sheet with DTAF labelled matrix, (b') with corresponding fluorescent image showing matrix (green) from scaffold-free sheet, and (b'') the merged image of (b) and (b'). (c) A light micrograph image of control mouse eye lacking a scaffold-free tissue sheet is shown, (c') with corresponding fluorescent image, and (c'') the merged image of (c) and (c'). Optical coherence tomography (OCT) was used to assess light scatter in the corneal stroma. (d) Cross-sectional projection image of untreated control mouse cornea. (e) Cross sectional image of a mouse eye with implanted tissue sheet (arrow) 1 week after implantation. (f) Cross-sectional projection image of mouse eye, 5 weeks after tissue sheet implantation. (g) Quantification of light scatter from OCT scans of the stroma showing light scatter by implanted tissue sheet 1-week post-implantation. (h) Quantification of light scatter from OCT scans of the stroma showing light scatter by implanted tissue sheet 5-weeks post-implantation.

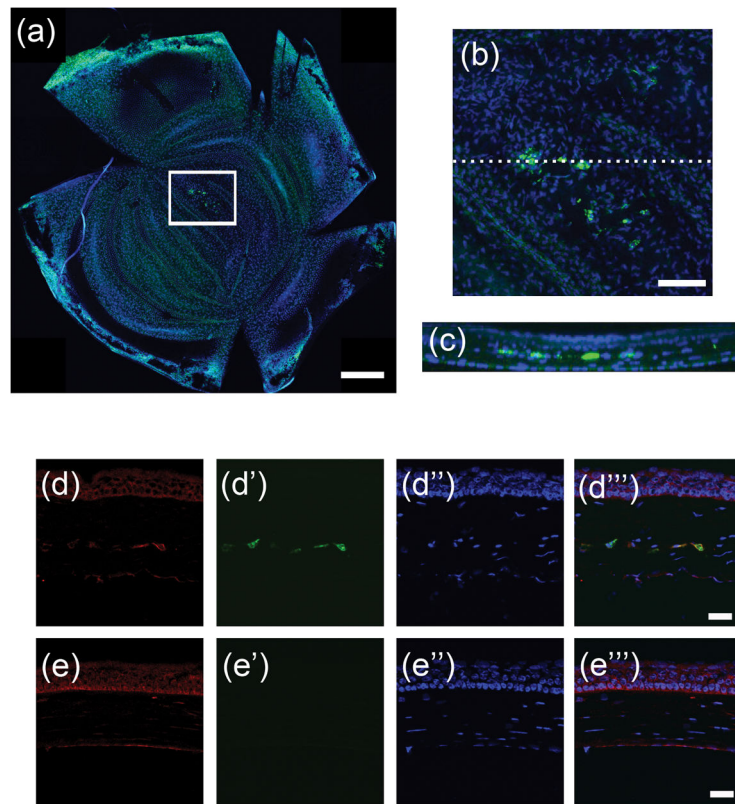


Figure 5. Persistence of human cells and matrix in mouse cornea stroma after implantation
 Five weeks after implantation of CSSC generated tissue sheets, mouse corneas were harvested and analyzed as described under Methods. (a) Confocal image of whole mount of cornea shows DiO labelled human cells (green). All cells were stained using nuclear dye DAPI (blue). (b) Higher magnification of boxed region in (a) shows region where human cells are located and in (c) a cross sectional projection of dotted line in (b) shows that the human cells are localized to the central stroma. (d) Immunostaining human keratocan (red) in cryosections from corneas 5 weeks after tissue sheet implantation. (d') Micrograph of green channel in same region as (d) shows DiO labelled human cells (green), (d'') micrograph of DAPI nuclear staining of all cells in same region as (d), and (d''') a merged image of (d)–(d'') show keratocan staining localization with respect to the human cells. (e) Immunostaining human keratocan (red) in a section of control mouse cornea lacking scaffold-free tissue sheets. (e') Micrograph of same region as (e) showing lack of DiO labeled green cells (green), (e'') micrograph in same region as (e) of DAPI nuclear staining of all cells (blue), and (e''') merged image of (e)–(e''). Scale bars: (a) = 500 μm , (b) = 100 μm , (d)–(e) = 20 μm